Assessment of Motion Planning Complexity for Rebar Placement Tasks Capturing Geometric, Spatial and Computational Aspects

Anantharaam R[1] , Bijo Sebastian[2] and Koshy Varghese[3]

[1] Master of Technology, Department of Civil Engineering, Indian Institute of Technology Madras, India
[2] Assistant Professor, Department of Engineering Design, Indian Institute of Technology Madras, India
[3] Professor, Department of Civil Engineering, Indian Institute of Technology Madras, India
ananthu_357@alumni.iitm.ac.in, bijo.sebastian@iitm.ac.in, koshy@iitm.ac.in

Abstract –

Robotic automation of rebar cage fabrication continues to face challenges due to its high spatial complexity, as dense reinforcement layouts, narrow clearances and irregular geometry restrict robot maneuverability. The groundwork for intelligent, perception-aware, and adaptable construction automation framework is missing in the literature. This research explores how the complexity of robotic rebar placement can be objectively quantified and assessed to inform automation strategies. A simulation-driven methodology is presented for calculating motion planning metrics, followed by clustering of tasks with similar complexity metrics. The results indicate that different cage configurations can be grouped based on their relative difficulty, providing clear insight into task feasibility as well as limitations. The motion planning workflow towards robotic rebar placement under different layouts was also validated over physical trials with a UR5 manipulator. These findings are crucial for enabling informed design and scheduling decisions in robotic cage fabrication workflows.

Keywords –

Construction Automation, Construction Robotics, Motion Planning, Complexity Assessment, Rebar Cage Assembly

1 Introduction

Most of the construction projects involve concrete work, reinforced with iron or steel bars to improve the strength characteristics [1]. However, the construction industry, being one of the least digitalized industries in the world [2], heavily depends on manual tying of such reinforcement elements. Oudah and El- Hacha [3] state that, being a key step in almost all the large-scale infrastructural projects, the progress of such reinforcement cage preparation activity directly relates to the completion time of the entire project. This high-intensity and time-consuming manual fabrication of reinforcement elements poses significant inefficiency, often resulting in project delays [4]. Also, the labor-intensive nature of the task introduces errors and variability, leading to quality deterioration. Apart from the productivity and quality standpoint, it is also proven that manual rebar tying is associated with Musculo-Skeletal Disorders (MSD) [1], which are chronic in nature.

Field observations conducted as part of this work indicated that the rebar cage fabrication activity consistently consumed the largest share of cycle time as shown in Figure 1, consuming 40% of the total cycle time.

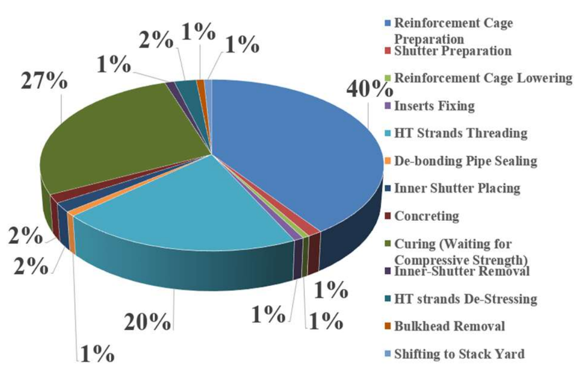

Figure 1. Activity-wise duration split-up

Results from the Productivity Measurement System (PMS) revealed that the actual productivity and production always fell short of what was actually planned as shown in Figure 2. This bottleneck in the initial stage of the production flow affects all the other activities downstream, thereby bringing down overall process efficiency.

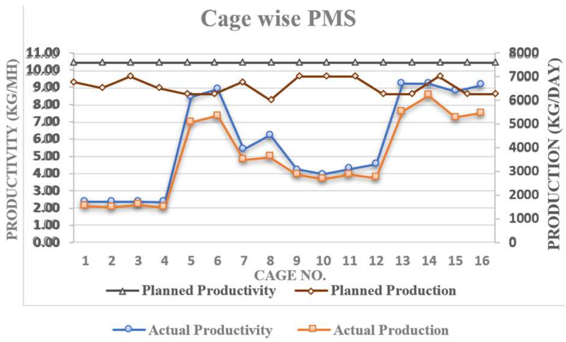

Figure 2. PMS analysis for cage fabrication activity

Automating the cage fabrication process could potentially solve some of the problems mentioned above. Persistent efforts to achieve this automation of cage fabrication has been observed in the literature. The body of knowledge ranges from the mechanization efforts of Safa et al [5] using automated rebar tying machines to reduce physical strain and improve productivity, to complete robotized production cell as proposed by Momeni et al [6] to fabricate the rebar cage, given the digital model of the cage. Jin et al [7] explored the use of crawler-mounted mobile robots to tie reinforcement elements. Recent studies revolve around more advanced robotic cage fabrication methods with mobile manipulators (Sun et al [8]) and fabrication of auxetic lattices for RC confinement (Schagen et al [9]).

However, the adoption of robotic solutions towards reinforcement cage fabrication brings up a new set of unique challenges. Unlike the rigid, well-defined components often encountered in assembly lines, rebars form intricate, three-dimensional lattices with varying geometry as shown in Figure 3.

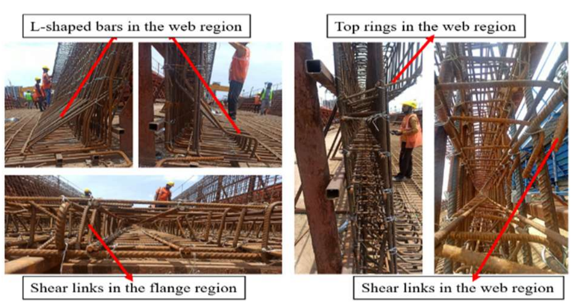

Figure 3. Highly cluttered rebar cage environment

Reinforcement lattices designed for human construction may not be best suited for robotic automation. In order to make the fabrication process efficient, Momeni et al [10] conducted research in determining the installation orders suitable for robotic fabrication.

However, the listed studies are largely limited to specific cage configurations and controlled setups, making them difficult to generalize or scale to diverse reinforcement layouts encountered in practice as described in Garg et al [11]. They primarily focus on task execution and sequencing, with limited emphasis on systematically characterizing the motion planning difficulty arising from varying geometric and spatial constraints. As a result, each new cage configuration introduces a different set of challenges, and there is a lack of a unified framework to evaluate and compare the complexity of robotic rebar placement across scenarios. It becomes important to assess the types of rebars that are difficult to place, as well as examine why they are difficult to place. This analysis will provide effective input for production cell design and operational plan. Quantifying the motion planning complexity for robotic rebar placement towards lattice construction can provide valuable insights towards redesigning the construction geometries and workcell configurations to better suit robotic automation.

Considering the limited existing research exploring this particular problem of motion planning complexity assessment, this study is performed with the following objectives:

1. Develop a methodology for quantifying the complexity of motion planning tasks associated with robotic rebar handling.
2. Implement the developed methodology to evaluate the motion planning complexity in a simulated environment.
3. Validate the practical applicability of the developed motion planning strategies through hardware validation.

In the following section, key motion planning algorithms and existing metrics for path assessment are reviewed, identifying the gaps that motivate the proposed complexity quantification methodology.

2 Review of Literature

In construction automation, particularly in tasks like rebar cage fabrication, effective motion planning remains under-explored. Although several studies have demonstrated robotic assembly in manufacturing settings, few have addressed the unique challenges posed by highly constrained construction environments.

Robotic motion planning has matured considerably with the advent of frameworks like MoveIt and libraries such as OMPL. Xu et al [12] demonstrated an integrated control system that couples coarse spatial planning (linear and circular primitives) with quintic‑spline joint interpolation to ensure smooth, collision‑free trajectories in cluttered workspaces. Similarly, Gümbel et al [13] leveraged RRT* and a sensitivity-based optimizer on a KUKA LWR iiwa - 14 arm to achieve both high repeatability and precise endpoint accuracy, illustrating how multi-objective routines can refine path quality in articulated manipulators. Liu et al [14] extended this benchmarking approach by chaining sampling-based planners (RRT, PRM) with optimization-based refiners (CHOMP, STOMP), finding that, while low complexity scenes yield consistently smooth trajectories, highly constrained environments still suffer from reduced success rates, highlighting the persistent challenge of narrow passages and tight clearances.

Beyond selecting and tuning motion planners, research aimed at measuring motion planning complexity is limited, especially for construction-related applications. Perille et al [15] introduced planner-agnostic terrain metrics (obstacle density, surface flatness, visibility) for mobile robots, but these global measures do not translate to multi-dof manipulators for applications such as rebar placement. Attali et al [16] proposed a visibility - based metric (LD+) that correlates well with RRT runtimes in abstract environments, yet focuses solely on the decision problem (path existence) and neglects kinematic constraints and object-specific factors. Human-inspired models, such as Yildirim et al's effort and risk estimator [17] for block rearrangement capture perceived difficulty but remain confined to primitive shapes and tabletop settings.

There is a clear gap in domain-specific quantification for construction tasks like rebar cage assembly, where (a) manipulator kinematics, (b) irregular bar geometries, and (c) severe spatial clutter converge. Existing metrics either overlook the robot's own reachability limits or fail to account for object shape and orientation. To fill this gap, this work presents a context-aware complexity framework, combining spatial and computational metrics, to objectively assess different rebars and cage configurations for motion planning applications.

3 Methodology Development

In order to assess the complexity of motion planning tasks in rebar cage fabrication, a three-stage methodology is proposed. To begin with, the motion planning metrics, which represent the spatial and computational complexity, are chosen and defined. The collected metrics are then grouped into meaningful clusters. Finally, the clusters are visualized to make meaningful classification and inference.

3.1 Proposed Metrics

The following five parameters are defined for the study:

3.1.1 Total Path Length (L)

The Total Path Length refers to the entire distance travelled by the centroid of the bounding box of the object being moved while traversing along the path generated by the motion planner from its start configuration to the goal configuration. It is measured as the sum of the Euclidean distances of the subsequent waypoints.

$$\mathrm{L} = \sum_{1=1}^{N-1} \|p_{i+1} - p_i\|_2 \tag{1}$$

where each waypoint $p_i \epsilon R^3$; represents the position of the centroid at a sampled pose along the path and $\|.\|_2$ denotes the Euclidean norm in meter squared. Spatial complexity for tasks such as rebar cage construction will force the planner to deviate from the straight line path between start and goal configurations as captured by the total path length metric.

3.1.2 Path Length Complexity Index (I_c)

The Path Length Complexity Index is calculated as the ratio of total path length (L) to the Euclidean straight line distance between the start and the goal configuration.

$$I_c = \frac{\sum_{1=1}^{N-1} \|p_{i+1} - p_i\|_2}{\sqrt{(x_{i+1} - x_i)^2 + (y_{i+1} - y_i)^2 + (z_{i+1} - z_i)^2}} \tag{2}$$

where $p_i = (x_i, y_i, z_i)$ is the i^{th} position along the planned path, making I_c a dimensionless index. A higher I_c indicates larger detours around obstacles, independent of absolute distances. Unlike total path length, which conflates long placements in large frames with genuinely complex trajectories, the I_c isolates environmental complexity.

3.1.3 Average Clearance from the obstacles (C_a)

C_a is the mean distance between the moving object and the closest obstacles along the planned path. It indicates the congestion of the work environment where the planner is working. Let c_i denote the minimum distance from the moving object to any obstacle in the environment:

$$C_a = \frac{1}{N} \sum_{i=1}^{N} c_i \tag{3}$$

where

$$\mathrm{c_i} = \min_{\mathrm{j \epsilon O}} \mathrm{dist}(\mathrm{p_i}, \mathrm{O_j}) \tag{4}$$

O $= \{O_1, O_2, \ldots, O_M\}$ is the set of all obstacle surfaces in the scene.

$dist(p_i, O_j)$ is the Euclidean or shortest distance from the point p_i to the obstacle O_j. The unit of measurement is metres.

3.1.4 Minimum Clearance from the Obstacles (C_m)

The minimum clearance from the obstacles refers to the smallest distance between any two collidable entities throughout the entire maneuver, indicating the narrowest spatial bottleneck.

$$C_m = \min_{i=1,\dots,N} c_i \tag{5}$$

It represents the most critical zone along the trajectory. The unit of measurement is metres.

3.1.5 Path Computation Time (T_c)

Path computation time measures the computational complexity of the motion planning problem. The unit of measurement is seconds (s). Even though this depends on the computational capability of the machine used, since the same machine is used for motion planning under all rebar placement tasks, it acts as an effective comparison metric, with longer planning times indicating harder configurations, often due to tight clearances or complex geometry.

The above five metrics together capture the spatial, geometric, and computational complexities of motion planning for rebar placement tasks under the cage fabrication task.

3.2 Data Collection through Simulation

The metrics for complexity assessment were calculated over simulations in the CoppeliaSim robotic simulator. STL (STereoLithogrpahy) files of the rebars were spaced and oriented to replicate partially-built rebar cage environments. A variant of Rapidly exploring Random Tree (RRT), named the RRTConnect algorithm, was used for motion planning in all the scenes. RRTConnect was chosen because of its simplicity, speed, and robustness in single-query high-dimensional planning tasks. RRTConnect grows two trees, from start and goal simultaneously, often finding a connection faster than single-tree planners. The data collection was done in two stages as explained below.

3.2.1 Stage I – Spatial Quantification

A pre-assembled rebar cage was assembled in the CoppeliaSim environment, except for the rebar object under study. The simulation scene setup is shown in Figure 4. The rebar object to be moved was made to spawn in a specified start location, and RRTConnect was called to perform motion planning in the C-space while avoiding the obstacles (already placed rebars), as shown in Figure 5. The following assumptions were made for the simulated scenes:

i. **Ideal perception and geometry:** The position, orientation, as well as geometry of each object is known a priori.

ii. **Static environment:** All the rebar cage elements remain rigid without any sagging, vibrations or shifts from their original position.

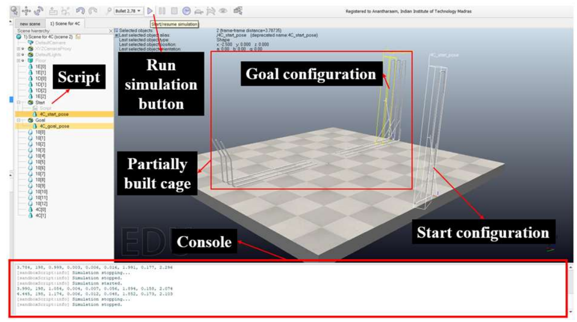

Figure 4. Scene setup for Spatial Quantification in CoppeliaSim

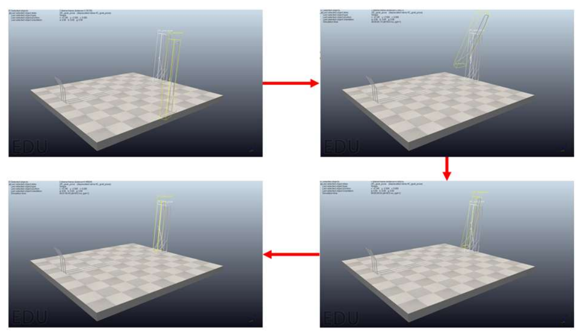

Figure 5. Spatial movement along the path planned by the RRTConnect

18 different simulated scenes were used for the metric calculation, with each scene repeated 100 times to account for the randomness of the RRTConnect motion planning algorithm. A maximum planning window of 20 seconds was allocated for each trial.

3.3 Stage II – Quantification with Manipulators

Similar to Stage I, in Stage II, partially built rebar cages were placed, and a 6-dof robotic manipulator was mounted on a dual-axes gantry to pick and place the rebar under study from initial locations as shown in Figure 6. A Kinova Jacoarm was used for the pick and place with an appropriate three-finger gripper. Along with the assumptions from Stage I, for Stage II, the robotic manipulator was assumed to have perfect control without any sensing errors. Five different scenes were modelled, with each scene made to run for 100 trials.

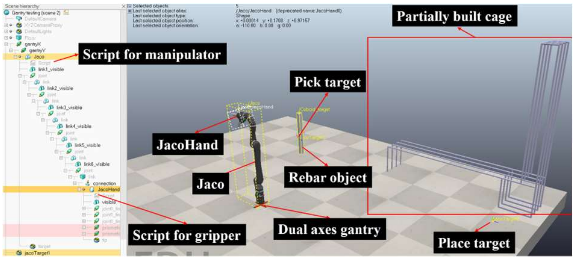

Figure 6. Scene setup for Stage II implementation

3.4 Data Analysis

The five motion planning metrics were computed for each trial in Stage I and Stage II. The values were then averaged to represent the difficulty profile for each placement scene. Once the raw metric values were obtained, they were min-max normalised as follows:

$$x_{norm} = \frac{x_i - x_{min}}{x_{max} - x_{min}} \quad (6)$$

where x_{norm} is the normalised value of a data point and x_{max}, x_{min} and x_i are the maximum, minimum and the i^{th} datapoint of the raw metrics. This is to ensure comparability across different units and magnitudes. For consistency in interpretation across all metrics, the normalised clearance metrics (average clearance and minimum clearance) were inverted such that lower clearances (more constrained environments) correspond to higher normalised values, aligning with the definition of increased motion planning complexity.

The normalised values were then subjected to K-means clustering in order to group the rebar placement scenes based on their difficulty profiles. The appropriate K-value (i.e., the number of clusters) was determined to be 3 by using the elbow method. The mean of the normalised values for each cluster was obtained as the characteristic value for the cluster.

3.5 Visualization

To aid in interpretation, the five-dimensional metric space was reduced using Principal Component Analysis (PCA) and the clusters were projected onto the principal-component plane for better visualization. A radar chart was prepared by projecting the normalised values on it, where each axis represents a defined motion planning complexity metric.

4 Results and Interpretations

The results from the simulated data collection are discussed in detail in this section. For the spatial analysis (Stage I), 18 rebar placement scenes are grouped into 3 clusters as visualised in Figure 7.

From the mean of normalized values, the clusters can be inferred as

Cluster 0 – EASILY PLACEABLE
Cluster 1 – MEDIUM DIFFICULTY
Cluster 2 – HIGHLY DIFFICULT

To visualize the metric-specific difficulty profile of each scene, a radar plot is presented in Figure 8.

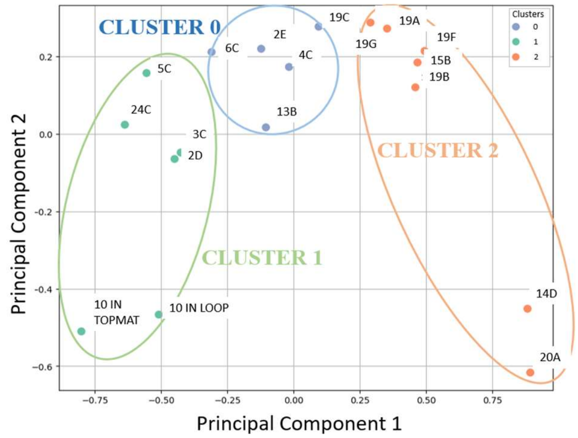

Figure 7. PCA plot for Stage I

Table 1. Mean of normalised values for Stage I

Cluster ID	L	I_c	C_a	C_m	T_c
0	0.340	0.390	0.027	0.159	0.201
1	0.863	0.812	0.115	0.435	0.530
2	0.752	0.390	0.901	0.936	0.901

Interpreting the spider plot in Figure 8 reveals the following findings:

- 3C and 4C bars (Figure 9 (a)), although complex in shape, are considered relatively easier, since they get placed in the initial stage of the cage making.

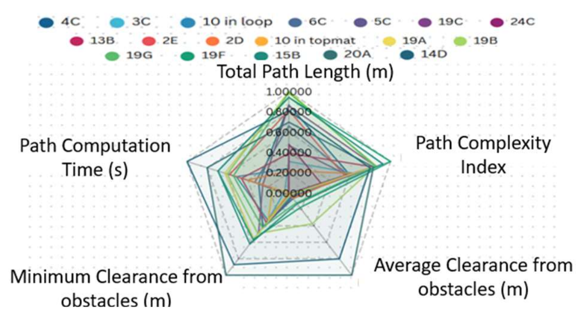

Figure 8. Radar plot for Spatial Quantification

- 19 series bars, as shown in Figure 9 (b), exhibited significant difficulty in their placement, as they need to be pushed through two sandwiched rebar layers.

- Rebar IDs 14D and 20A, as shown in Figure 9 (c) and Figure 9 (d), are the most difficult to place since they are heavily constrained in spatial layout.

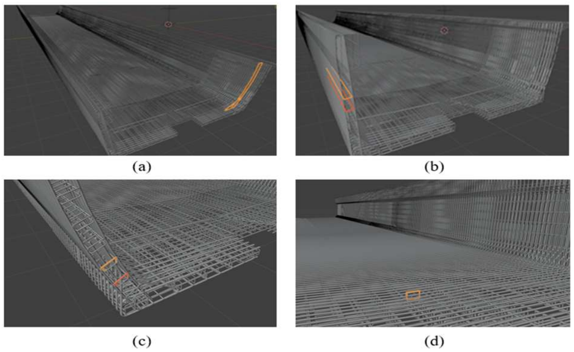

Figure 9. STL representations of rebar ids of a U-girder - (a) rebar ID 4C, (b) rebar ID 19 series, (c) rebar ID 14D, (d) rebar ID 20A

The five scenes from Stage II are divided into 3 clusters as shown in the PCA plot in Figure 10. These results also provided some interesting findings. Although there are three clusters, the means of the normalized values show that cluster 1 and cluster 2 represent different profiles of difficulty. While cluster 1 tops in the first two parameters, indicating longer paths to place the rebars, cluster 2 tops the chart in the last three parameters, showing its difficulty in constricted spatial zones. The radar plot also reveals this insight visually, as shown in Figure 11.

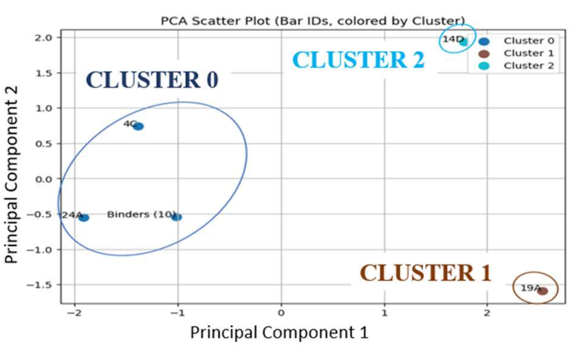

Figure 10. PCA plot for Stage II

Table 2. Mean of normalised values for Stage I

Cluster ID	L	I_c	C_a	C_m	T_c
0	0.069	0.123	0.171	0.519	0.164
1	1.000	1.000	0.234	0.917	0.702
2	0.164	0.377	1.000	1.000	1.000

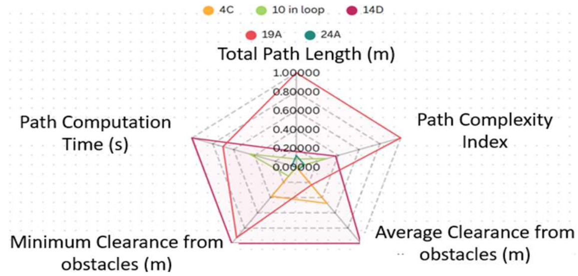

Figure 11. Radar plot for Stage II

Yet another important observation is the comparison between Stage I and Stage II, revealing the quantum of complexity that the addition of a robotic manipulator brings. The parameter-wise comparison of the two stages is shown in Figure 12.

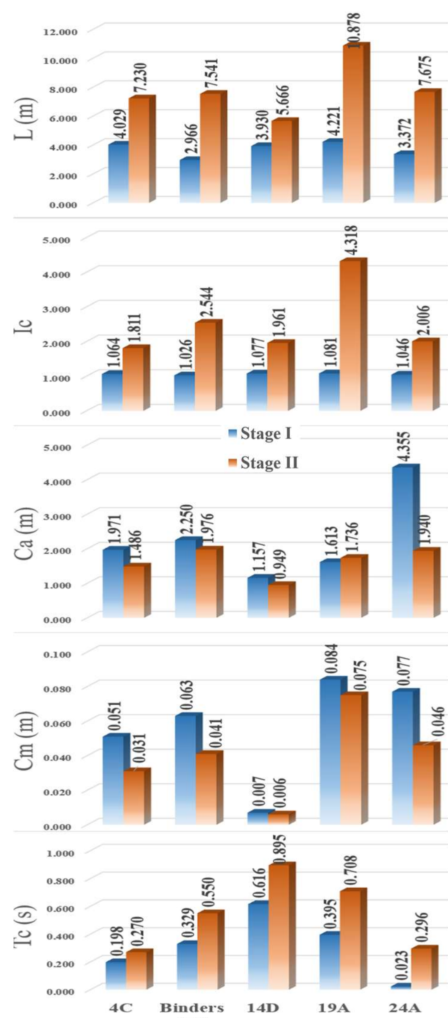

Figure 12. Parameter comparison between Stage I and Stage II

The charts reveal that there is a significant surge in the parameter values on introducing a robotic manipulator into the scene. This is due to the added constraints in terms of joint limits, reachability and the possibility of self-collision for the robot.

5 Hardware Implementation and Validation

To verify the simulation-based complexity, the developed methodology was tested with a 6-dof UR5 robotic manipulator, with a Robotiq 3-fingered adaptive gripper. The use of a UR5 platform for hardware validation, in place of the Kinova Jaco arm used in Stage II simulations, is supported by their comparable effective payload capacities (~1.6–1.8 kg considering gripper integration) and similar 6-DOF kinematic structure and workspace scale, ensuring consistency in motion planning behaviour.

Experimental scenes were set up in the laboratory with scaled-down rebar pieces and corresponding obstacle objects. Three scenes of varying complexity levels were set up to imitate the respective rebar placements of rebar ids 4C, 19C and 14D (Figure 9) as shown in Figure 13, Figure 14 and Figure 15. The motion planner RRTConnect was called from OMPL through the MoveIt interface, and the robotic motions are monitored in real-time using RViz. The data was collected as rosbags and processed later to obtain the metrics.

Figure 13. Physical Experimentation - Scene 1

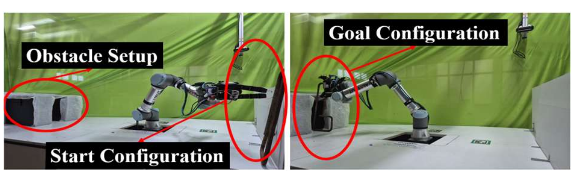

Figure 14. Physical Experimentation - Scene 2

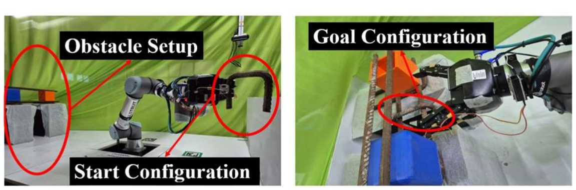

Figure 15. Physical Experimentation - Scene 3

Ten trials were conducted for each scene. The results from the physical trials, as shown in Table 3 indicate that the Scene 2 stands as the most complex. These results from the hardware validation fall close to the simulated Stage II results, classifying the sliding placement of 19 series rebars to be more complex than placing the 4C rebars (Figure 9).

Table 3. Normalized results of Hardware Validation

Scene ID	L	I_c	C_a	C_m	T_c
Scene I	0.000	0.000	0.734	0.000	0.046
Scene II	1.000	1.000	1.000	0.237	1.000
Scene III	0.367	0.367	0.000	1.000	0.000

To validate the results, the same three scenes were modelled in CoppeliaSim, and the results from the physical experimentation and the simulation were compared. The results, as shown in Figure 16, indicate that the trends across scenes showed a similar pattern.

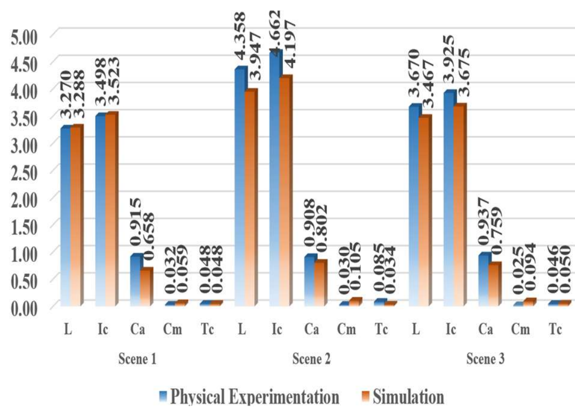

Figure 16. Comparison between Physical Experimentation and Simulation Replicas

6 Discussion and Conclusion

This study has demonstrated a practical framework for quantifying motion planning complexity in robotic rebar placement, revealing clear patterns across both purely spatial and manipulator-based scenarios. The manipulator-based simulation and experimental validation demonstrated kinematic reachability and joint limits, exacerbating spatial challenges in rebar placement. Distinct difficulty profiles with combinations of path detours, clearance margins, and planning times were observed. These patterns aided in classifying each rebar placement task into clusters, informing which aspect of the placement needs to be taken care of during the production cell design.

The study did not involve perception-based real-time motion planning and grasping constraints. The future works look forward to integrating these components to refine the proposed methodology. The insights from such studies would be pivotal for automated cage fabrication as they enable data-driven planner selection (e.g., favouring rapid sampling for geometrically complex cases or cautious, sensor-guided motion in tight spaces), informed cell layout (optimizing access to bars with high-difficulty profile), and realistic throughput estimations. As construction robotics transitions from laboratory demonstrations to site-ready automation, such complexity-aware planning frameworks will be essential for bridging the gap between algorithmic feasibility and production-level reliability.

Acknowledgement

The first author thanks Larsen and Toubro (L&T) for support through the Build India Scholarship programme. The authors acknowledge the support of L&T Heavy Civil Infrastructure IC for supporting the broader aspects of this work.

References

[1] P. Vi. A field study investigating the effects of a rebar-tying machine on trunk flexion, tool usability and productivity. *Ergonomics*, 49(14):1437–1455, 2006.

[2] X. Tan, L. Xiong, W. Zhang, Z. Zuo, X. He, Y. Xu, and F. Li. Rebar-tying robot based on machine vision and coverage path planning. *Robotics and Autonomous Systems*, 182:104826, 2024.

[3] F. Oudah and R. El-Hacha. Joint performance in concrete beam-column connections reinforced using SMA smart material. *Engineering Structures*, 151:745–760, 2017.

[4] R. Feng, Y. Jia, T. Wang, and H. Gan. Research on the system design and target recognition method of the Rebar-Tying robot. *Buildings*, 14(3):838, 2024.

[5] M. Safa, J. G. Cardenas, D. G. Leblanc, D. Rose, and A. Shahi. Improving construction labour productivity using automatic rebar tying gun. In *Proceedings of the 33rd International Symposium on Automation and Robotics in Construction (ISARC)*, pages 1–9, Auburn, USA, 2016.

[6] M. Momeni, J. Relefors, A. Khatry, L. Pettersson, A. V. Papadopoulos, and T. Nolte. Automated fabrication of reinforcement cages using a robotized production cell. *Automation in Construction*, 133:103990, 2021.

[7] J. Jin, W. Zhang, F. Li, M. Li, Y. Shi, Z. Guo, and Q. Huang. Robotic binding of rebar based on active perception and planning. *Automation in Construction*, 132:103939, 2021.

[8] Sun, T., B. Han, J. Wu, S. Rusinkiewicz, and Y. Shao. 2025. Mobile robotic rebar cage assembly via imitation learning. *Automation in Construction*, 181:106671, 2025.

[9] Schagen, B., T. Vitalis, A. Thoma, T. Bhave, M. Pacher, D. Blank, and S. Gerasimidis. 2026. Robotic fabrication of structural steel architected auxetic lattices for reinforced concrete confinement. *Structures*, 86:111355, 2026.

[10] Momeni, M., J. Relefors, L. Pettersson, A. V. Papadopoulos, and T. Nolte. 2022. On the Bar Installation Order for the Automated Fabrication of Rebar Cages. In *Proceedings of the 39th International Symposium on Automation and Robotics in Construction (ISARC),* pages 508–511, Bogotá, Columbia, 2022.

[11] Garg, A., and V. R. Kamat. 2013. Virtual prototyping for robotic fabrication of rebar cages in manufactured concrete construction. *Journal of Architectural Engineering*, 20 (1), 2013.

[12] T. Xu, H.-Z. Liu, R. Huang, Z. Yao, and J.-Y. Xu. Research on Motion Trajectory Planning of industrial robot based on ROS. In *Proceedings of the 6th International Conference on Automation, Control and Robotics Engineering (CACRE)*, pages 58–62, Xi'an, China, 2022.

[13] P. Gümbel, X. He, and K. Dröder. Precision optimized pose and trajectory planning for vertically articulated robot arms. *Procedia CIRP*, 106:185–190, 2022.

[14] S. Liu and P. Liu. Benchmarking and optimization of robot motion planning with motion planning pipeline. *The International Journal of Advanced Manufacturing Technology*, 118(3–4):949–961, 2021.

[15] D. Perille, A. Truong, X. Xiao and P. Stone. Benchmarking metric ground navigation. In *Proceedings of the IEEE International Symposium on Safety, Security, and Rescue Robotics (SSRR)*, pages 116–121, Abu Dhabi, UAE,2020.

[16] A. Attali, S. Ashur, and M. N. Amato. Measuring Guidance for the Motion Planning Decision Problem. In *Proceedings of the 34th International Conference on Automated Planning and Scheduling*, Workshop on Planning and Robotics (PlanRob), Alberta, Canada, 2024.

[17] I. Yildirim, B. Saeed, G. Bennett-Pierre, T. Gerstenberg, J. B. Tenenbaum, and H. Gweon. Explaining intuitive difficulty judgments by modeling physical effort and risk. In *Proceedings of the 41st Annual Conference of the Cognitive Science Society (CogSci)*, 1233, Montreal, Canada, 2019.